Tackling polypharmacology of kinase inhibitors by transcription factor activity profiling.

Alexander V. Medvedev[1], Sergei Makarov Jr. [1], Lyubov A. Medvedeva[1], Elena Martsen[1], Kristen L. Gorman[1], Benjamin Lin[1], Sergei S. Makarov[1,*].

[1]Attagene Inc., 7020 Kit Creek Rd, Morrisville NC 27560

*Corresponding author

smak@attagene.com

tel 919-270-6031

ABSTRACT.

Protein kinase inhibitors (PKI) evolved as promising drugs for multiple diseases. However, PKIs' promiscuity causes polypharmacological effects challenging therapeutic development. We show that the polypharmacology of PKIs can be inferred from their impact on transcription factors (TF) lying at the apexes of signaling pathways. Using a high-content reporter assay, we evaluated TF activity profiles (TFAP) in cells treated with Akt, CDK, Aurora, Raf, MEK, and ERK inhibitors. In each case, we found kinase-specific consensus TFAP signatures signifying the on-target PKI activity. Remarkably, proximal kinases had the highest similarity values of their PKIs' consensus signatures. Furthermore, we show that individual PKIs exhibited the consensus, "on-target signatures" within certain "specificity windows" and distinct "off-target signatures" at other concentrations. We also show that the off-target PKI signatures permit pinpointed the underlying biological effects. Therefore, the TFAP approach provides clear-cut quantitative metrics for assessing the dominant PKI activity and concentration ranges where the on-target activity dominates cell response. Thus, this effect-based approach illuminates PKI biology invisible to target-based techniques streamlining the selection of kinase chemical probes and PKI drug prioritization.

INTRODUCTION.

Protein kinases evolved as the most important drug targets for cancer1,2, and kinase drug discovery is rapidly expanding into immunological, inflammatory, degenerative, metabolic, cardiovascular, and infectious diseases3. One of the most challenging issues in therapeutic development is PKI promiscuity stemming from a significant homology of the active kinase centers5,6. Genome-wide profiling studies 5,13–15 revealed that even the most selective PKIs act on multiple kinases. Furthermore, like other drugs, PKIs can interact with a plethora of non-kinase effectors, such as bromodomain-containing proteins, cytoskeleton, prostaglandin synthases, the AHR receptor, ferrochelatase, and NQO216.

The multiple PKI interactions produce polypharmacological effects, posing difficult questions to drug developers. On the one hand, PKI polypharmacology can compromise drug safety, but it can also increase the therapeutic efficacy. Furthermore, PKI polypharmacology complicates the selection of chemical probes for elucidating the kinases' functions and target validation. The existing PKI evaluation techniques are focusing on profiling the PKI binding/inhibitory activity across kinases; however, these target-based approaches do not provide clear guidance for prioritizing drug candidates and chemical probe selection.

Here, we present an orthogonal, effect-based approach for the biological evaluation of PKIs. This approach entails assessing PKIs' impact on the cellular network of signal transduction pathways that regulate gene expression. As a readout, we evaluate the activity of transcription factors (TFs) that lie at the apexes of signaling pathways and connect them to regulated genes. Thus, by profiling TFs' activity we can capture the response of the cellular signaling betwork.

Our approach is based on the premise that protein kinases lie at the heart of signal transduction pathways. Furthermore, as we demonstrated previously, TF activity profiles (TFAP) permit pinpointing perturbed biological processes and cell systems.

Here, we examined TFAP signatures for inhibitors of Akt, Aurora, cyclin-dependent kinases (CDKs), Raf, MEK, and ERK kinases. To do that, we used our high-content reporter assay (the FACTORIAL) enabling a parallel evaluation of multiple TFs in a single well of cells.

We show that the TFAP evaluation provides clear quantitative metrics for evaluating PKI polypharmacology. Specifically, the TFAP signatures permit assessing the cumulative biological effects of PKIs the on-target and off-target PKI activity, and the concentration ranges where these activities dominate. Thus, this effect-based approach complements the existing, target-based techniques, streamlining chemical probe development and kinase drug prioritization.

RESULTS.

Profiling TF activity by the FACTORIAL assay. The FACTORIAL is a high-content reporter assay enabling a parallel assessment of multiple TFs in a single well of cells11. The assay comprises TF-responsive reporters termed reporter transcription units (RTUs) largely identical to traditional reporter gene constructs. However, the RTU activity is evaluated by their transcription.

The assay workflow entails transient transfection of RTU plasmids into assay cells and profiling the RTU transcripts. We used a homogeneous RNA detection proviving equal detection efficacy across the RTUs11 (Fig. S1). As shown previously, this approach drastically reduces the influence of experimental variables, ensuring exceptionally reproducible TF activity profiles (TFAP)11.

The endpoints of FACTORIAL-generated TFAP signatures encompass TF responses to various stimuli, including xenobiotics, growth factors, inflammation, and various stresses (listed by Fig. S1).

Assessing PKI TFAP signatures. The TFAP signatures of PKIs are presented as radial graphs showing TF activity fold changes in drug-treated vs. vehicle-treated cells. By this definition, the TFAP signature of vehicle-treated cells is a perfect circle (the “null” signature). Each presented here TFAP signature is an average of three independent FACTORIAL assays.

To assess the pair-wise similarity of TFAP signatures, we use Pearson correlation coefficient ***r***. The signatures with the similarity r>0.70 are considered identical because the probability of two random 47-endpoint signatures correlating with r> 0.70 is extremely low. In addition, we calculated the Euclidean distance ***d*** from the null signature to discriminate the experimental noise. The signatures with ***d***<0.15 were considered the null signature.

We used a diverse panel of inhibitors of Akt, cyclin-dependent kinases (CDK), Aurora, Raf, MEK, and ERK kinases in a concentration-response format. The TFAP signatures were subjected to cluster analysis to identify the consensus signatures.

The consensus signature of AKT inhibitors. The Akt1, Akt2, and Akt3 kinases mediate cell responses to various stress stimuli and growth factors. This kinase family plays a critical role in multiple cellular processes such as glucose metabolism, apoptosis, cell proliferation, and migration.

The FACTORIAL analysis of four pan-Akt ATPase inhibitors and one allosteric Akt 2/3 inhibitor showed a consensus TFAP signature (exemplified by Fig. 1A, see also supplementary Fig. S2 for more data on other Akt inhibitors). Importantly, Akt inhibition by a kinase-dead Akt mutant cDNA (Akt K179M) also produced the consensus TFAP signature (Fig. 1A).

The consensus signature comprised multiple endpoints, including known TF targets of Akt (b-catenin/TCF, IRFs, NF-kB, and p53). Therefore, regardless of the mode of action and the specific kinase targets within the Akt family, Akt inhibitors exhibited a distinct consensus signature signifying their on-target activity.

The consensus signature of CDK inhibitors (Fig. 1B). Cyclin-dependent kinases (CDK) comprises multiple kinases controlling the cell cycle and are also involved in regulating mRNA transcription and processing. CDKs' activity is modulated by the binding of regulatory proteins called cyclins and it can be further modulated by phosphorylation and other binding proteins, e.g. p27.

The analysis of 13 CDK inhibitors with different selectivity profiles for individual CDK kinases revealed a consensus signature with multiple TF endpoints (Fig. 1B, see also Fig. S3 for more inhibitors' data). Therefore, CDK inhibitors had a consensus signature, regardless of their specific kinase targets within the CDK family.

The consensus signature of Aurora inhibitors (Fig. 1C). Aurora kinases A, B, and C play a crucial role in cellular division by controlling chromatid segregation. The evaluation of five Aurora ATPase inhibitors with different selectivity profiles showed a consensus signature (Fig. 1C, see also supplementary Fig. S4), regardless of their specific kinase targets within the Aurora family.

The consensus signatures of Raf, MEK, and ERK inhibitors. Mitogen-activated protein kinase (MAPK) cascades regulate cell proliferation, survival, and differentiation. One of those pathways is the extracellular signal-regulated kinase (ERK) MAPK pathway is considered a particularly important player in oncogenesis.

The ERK MAPK pathway constitutes Raf kinases that phosphorylate and activate downstream MAPK/ERK kinases (MEK)1/2 that, in turn, activate ERK1/2 kinases. An important role for the Raf/MEK/ERK cascade in oncogenesis is evidenced by mutational activation of Raf in many cancers. Additionally, the Raf/MEK/ERK pathway is a key downstream effector of the Ras GTPase, the most frequently mutated oncogene in human cancers.

Testing the panel of five pan-Raf inhibitors and two B-Raf inhibitors revealed a consensus TFAP signature (Fig. 2A, see also Fig. S5). Furthermore, we also found consensus signatures for inhibitors of the downstream MEK1/2 and ERK1/2 kinases (Fig. 2B,C and Figs. S6 and S7). Remarkably, the consensus signatures of Raf, MEK, and ERK inhibitors had a high-degree similarity. The endpoints of these signatures were consistent with known TF targets of the Raf/MEK/ERK pathway, e.g., AP-1 and NRF2.

Proximal kinases have the highest similarity of the consensus PKI signatures. Cluster analysis of the consensus PKI signatures for the evaluated kinase families has shown that kinases of the same cascade (Raf, MEK, and ERK) had the highest similarity

of their consensus PKI signatures (Fig. 3), In fact, the pairwise similarity values of the consensus Raf, MEK, and ERK PKI signatures exceeded the identity threshold (r>0.70). in contrast, distant kinases (CDK, Aurora, and Akt) had a low-degree similarity (Fig. 3).

The TFAP-based assessment of PKI polypharmacology. The screening of individual inhibitors showed that their TFAP signatures matched the consensus PKI signature only within certain concentration ranges that we termed the “specificity windows”. At other concentrations, we observed distinct, “off-target signatures” with a low similarity (r<0.70) to the consensus signatures. To identify the underlying effects of the off-target signatures, we interrogated our TFAP database of reference perturbagens. The following data exemplify this approach (Figs. 4-6).

CDK inhibitors. Fig. 4 shows TFAP signatures of CDK inhibitors Dinaciclib and NU6140. Dinaciclib is an inhibitor of CDK2, CDK5, CDK1, and CDK9 kinases with nanomolar IC50 values in a cell-free assay. NU6140 was developed as a selective CDK2 inhibitor with IC50 of 0.4 uM.

Dinaciclib showed the consensus CDK PKI signature at all tested concentrations (30 nM to 20 uM) (Fig. 4A). In contrast, the NU6140 signatures matched the consensus CDK PKI signature only at the highest tested concentration (6.7 uM); at lower concentrations, its signatures matched the consensus signature of Aurora inhibitors (Fig. 4B). These data agreed with the reported NU6140 activity at Aurora A/B kinases (IC50 of 67 and 35 nM, respectively) (Jorda). Therefore, cell response was dominated by Aurora inhibition at low concentrations of NU6140 and by CDK inhibition at higher concentrations.

Akt inhibitors. Fig. 5 shows TFAP signatures of Akt inhibitors GDC0068 and A674563. GDC-0068 (a.k.a. Ipatasertib and RG7440) is a selective pan-Akt inhibitor targeting Akt1/2/3 with IC50 of 5 nM/18 nM/8 nM in cell-free assays. A674563 is a multi-kinase inhibitor of Akt1 (IC50 of 11 nM in cell-free assays), PKA, Cdk2 (IC50 of 16 nM and 46 nM) (Chomer), and FLT3 (IC50=2.1 uM) (Wang).

The GDC0068 signatures were identical to the consensus Akt PKI signature at all tested concentrations (60 nM to 15 uM) (Fig. 5A). In contrast, A674563 signatures were dissimilar to the Akt PKI consensus signature but had a high similarity to the consensus CDK PKI signature (Fig. 5B). Therefore, the dominant biological effect of A674563 was defined by CDK inhibition.

ERK inhibitors. Fig. 6 shows TFAP signatures of ATP-competitive ERK inhibitors GDC0094 and Ulixertinib. GDC-0994 (a.k.a. Ravoxertinib) is an ERK1/2 inhibitor with IC50 of 1.1 nM and 0.3 nM, respectively. Ulixertinib (BVD-523; VRT752271) is a reversible ERK1/2 inhibitor with IC50 of <0.3 nM at ERK2 also inhibiting RSK kinase.

The GDC-0994 signatures were identical to the consensus ERK PKI signature at concentrations ranging from 30 nM to 2.2 uM (Fig. 6A). However, at a higher concentration (6.7 uM), the GDC-0994 signature had a high similarity to the consensus signature of histone deacetylase (HDAC) inhibitors (ref.)).

The Ulixertinib signatures were identical to the consensus ERK PKI signature at concentrations from 30 nM to 250 nM (Fig. 6B). At the concentration of 2.2 uM, the Ulixertinib signature was identical to the Raf PKI consensus signature; at 6.7 uM, it matched the consensus TFAP signature of the mitochondria ETC inhibitors (ref.).

Therefore, the off-target TFAP signatures suggested an HDAC inhibitory activity of GDC-0994 and mitochondria inhibition by Ulixertinib. Functional assays have confirmed these predictions (Fig. S8). Therefore, the TFAP approach permits assessing PKI activity at non-kinase effectors.

Evaluating PKIs as chemical probes. A chemical kinase probe is a selective small-molecule modulator of kinase activity. These probes are indispensable for delineating the mechanistic and phenotypic effects of kinases in cell-based and animal studies (ref.) and drug target validation (sweis). Chemical probes must be active in cells and satisfy other quality criteria, such as selectivity and chemical stability (Arrowsmith et al., 2015; Blagg and Workman, 2017; Edwards et al., 2009; Bunnage et al., 2013). Another essential parameter is the concentration range wherein cell response is defined by the probe's specific activity toward the target kinase.

The TFAP approach offers a straightforward solution for assessing chemical kinase probes. Since inhibitors of the same kinase family, regardless of their MOA have a consensus signature, this consensus signature provides a marker for the on-target PKI activity. Furthermore, the consensus PKI signatures of individual inhibitors exist only within certain concentration ranges (the "specificity windows"), transforming into distinct signatures at other concentrations, Thus, the "specificity windows" provide quantitative metrics for determining appropriate concentration ranges of chemical probes.

Fig. 7 illustrates this evaluation approach for Akt and MEK inhibitors. Among Akt inhibitors, GDC 0068 had the largest specificity window (Fig. 7A). Among MEK inhibitors, Binimetinib and Selumetinib showed the largest specificity windows (Fig. 7B). Our data agree with the Chemical Probes Portal that also proposes Selumetinib as a chemical probe for MEK (ref.). Therefore, TFAP-based evaluation provides clear-cut criteria for selecting chemical kinase probes.

DISCUSSION.

In this work, we have described an effect-based PKI evaluation approach that entails profiling the responses of cellular signaling pathways. As the readout, we assessed the activity of transcription factors lying at the signaling pathways' apexes. Using a high-content reporter assay (the FACTORIAL), we characterized cell response by quantitative signatures (TF activity profiles). We examined the PKI TFAP signatures at a late (24 h) time point to obviate PKI's transient effects and different pharmacokinetics. The main findings are as follows:

1. We found that different Inhibitors of the same kinase, regardless of their mode of action, shared a consensus TFAP signature. An example is the consensus signature of ATP-competitive and allosteric Akt inhibitors and the kinase-dead Akt mutant (Figs. 1A and S2).

Therefore, we concluded that kinase inhibition causes coordinated changes in signaling pathways' activity, epitomized by the consensus PKI signature. Thus, this consensus signature appears a bona fide marker for the PKI on-target activity.

2. We found distinct PKI consensus signatures for CDK, Aurora, Raf, ERK, and MEK (Figs. 1-2). Therefore, the kinase-specific PKI TFAP signatures are a general phenomenon for multiple kinase families of the human kinome.

3. We found that proximal kinases of the same kinase cascade (Raf/MEK/ERK) had high-similarity PKI consensus signatures, distinguishing them from distal kinases (Fig. 3). This observation further supports consensus PKI signatures as the on-target activity markers. Furthermore, these data suggest that PKI consensus signatures may help place poorly characterized "dark kinases" into the framework of the illuminated kinome.

4. Individual PKIs' signatures matched the consensus PKI signature only within certain concentration ranges (Figs. 4-8). Therefore, within the "specificity window," cell response to a PKI is defined by its on-target activity. At other concentrations, we observed distinct signatures indicating off-target PKI activities. What is essential, the off-target PKI signatures allowed us to identify the underlying PKI activity by interrogating the TFAP signatures of reference perturbagens. Therefore, the TFAP evaluation produces clear quantitative metrics (the on-target consensus PKI signature, the specificity window, and the off-target signatures) for PKI bioactivity assessment.

One important application of the TFAP approach is evaluating PKI chemical probes. We showed that concentration-response TFAP assessments provided clear-cut criteria for selecting appropriate concentrations for PKI chemical probes (Fig. 7). Moreover, as the TFAP signatures are generated by a prolonged PKI incubation in assay cells, our approach also addresses other essential probe parameters, i.e., activity in cells, biotransformation, and chemical stability.

Another application of the TFAP approach is the evaluation of kinase drugs. PKI polypharmacology can compromise drug safety, but it can also significantly potentiate therapeutic efficacy. In this regard, our approach allows assessing PKI concentrations for the on-target activity along with the off-target effects on other kinases and non-kinase effectors.

Previously, we showed that perturbations of various biological processes and cell systems produced characteristic TFAP signatures. We found specific signatures for several perturbagens' classes, including mitochondria and Ub/PS inhibitors, DNA damaging agents, and cytoskeleton disruptors. The present work shows that kinase inhibitors, too, have kinase-specific TFAP signatures. Therefore, the TFAP approach enables a comprehensive biological evaluation of uncharacterized chemicals.

A distinct advantage of the TFAP approach is that it describes cells' responses by well-defined quantitative signatures that permit directly comparing compounds' bioactivity without complicated bioinformatic analyses needed by other systems biology approaches (e.g., transcriptomics).

One caveat of our signature-based PKI evaluation is that it may not have sufficient resolution for distinguishing inhibitors of some proximal kinase families. In this regard, the assay resolution can be further improved by including additional TF reporters in the FACTORIAL assay. Akin to that, inhibitors of different kinases of the same kinase family have identical TFAP signatures. This limitation can be overcome using the PKI selectivity profiling data by target-based techniques.

In summary, the effect-based TFAP approach illuminates PKI biology invisible to existing target-based evaluation techniques. Thus, this orthogonal approach expands the kinase research toolbox, facilitating chemical kinase probe evaluation and drug development.

FIGURE LEGENDS.

Fig. 1. The consensus TFAP signatures of Akt (A), CDK (B), and Aurora (C) inhibitors. The PKIs (*left panels*) were evaluated by the FACTORIAL assay in human hepatocyte HepG2 cells in a concentration-response format (a 24-h incubation). Each TFAP signature is an average of three independent FACTORIAL assays. The PKI TFAP signatures were analyzed by unsupervised hierarchical cluster analysis to identify the consensus signatures. The similarity values for the consensus and individual PKI signatures were calculated as the Pearson correlation coefficient ***r*** (*left panels*). The *central panels* show the consensus PKI signatures (in blue) overlaid by the signatures of individual PKIs (in red). The TFAP signatures' axes show fold-change TF activity values in PKI-treated vs. vehicle-treated cells (on a log scale). *The right panel:* The TFAP signatures' endpoints (see supplementary Fig. S1 for a detailed description).

Fig. 2. The consensus TFAP signatures of Raf (A), MEK (B), and ERK (C) inhibitors. The PKIs were evaluated as described by Fig. 1 legend.

Fig. 3. The similarity of consensus PKI signatures correlates with kinases' proximity. The clustering tree shows the similarity values for the consensus PKI signatures of indicated kinases. The signatures were analyzed by unsupervised hierarchical cluster analysis. The similarity of the signatures calculated as Pearson correlation coefficient ***r***.

Fig. 4. The TFAP-based assessment of CDK inhibitors' polypharmacology. The PKIs' TFAP signatures were obtained as described by Fig. 1 legend. **A.** The TFAP signatures of Dinaciclib (in red) at indicated concentrations overlayed on the consensus CDK PKI signature (in blue). **B.** The TFAP signatures of NU 6140 (in red) at indicated concentrations overlayed on the consensus CDK (upper panel) and Aurora (bottom panel) PKI signatures. The similarity of the overlaid signatures calculated as Pearson correlation coefficient ***r***. Each TFAP signature is an average of three independent FACTORIAL assays.

.

Fig. 5. The TFAP-based assessment of Akt inhibitors' polypharmacology. The PKIs' TFAP signatures were obtained as described by Fig. 1 legend. **A.** The TFAP signatures of GDC 0068 (in red) at indicated concentrations overlayed on the consensus Akt PKI signature (in blue). **B.** The TFAP signatures of A 674563 (in red) at indicated concentrations overlayed on the consensus Akt (upper panel) and CGK (bottom panel) PKI signatures. The similarity of the overlaid signatures calculated as Pearson correlation coefficient ***r***. Each TFAP signature is an average of three independent FACTORIAL assays.

Fig. 6. The TFAP-based assessment of ERK inhibitors' polypharmacology. The PKIs' TFAP signatures were obtained as described by Fig. 1 legend. **A.** The TFAP signatures of GDC 0094 (in red) at indicated concentrations overlayed on the consensus ERK PKI signature (at 0.03 to 2.2 uM) or the consensus signature of HDAC inhibitors (at 6.6 uM) (in blue). **B.** The TFAP signatures of Ulixertinib (in red) overlayed on the consensus ERK PKI signature (upper panel). Bottom panel: The Ulixertinib signatures (red) overlaid on the consensus signatures of Raf or mitochondria ETC inhibitors (blue).

The similarity of the overlaid signatures calculated as Pearson correlation coefficient ***r***. Each TFAP signature is an average of three independent FACTORIAL assays.

Fig. 7. Evaluating PKI chemical probes. The graphs show the similarity values (Pearson correlation ***r***) of PKI TFAP signatures vs. the consensus signatures of Akt (A) and MEK (B) inhibitors. The similarity thresholds (in grey) are set at r=0.70. The specificity windows (in green) indicate PKI concentrations for the on-target activity. Off-target concentrations are shown in red. Each graph is an average of three independent FACTORIAL assays.

A AKT

PKI	Target	MOA	[C], uM	Corr. *r*
Afuresertib	pan-AKT	ATP	0.25	**0.94**
AZD 5363	pan-AKT	ATP	0.06	**0.89**
GDC-0068	pan-AKT	ATP	0.19	**0.90**
GSK690693	pan-AKT	ATP	0.74	**0.86**
MK-2206	AKT 2,3	Allost.	2.20	**0.79**

B CDK

PKI	Target	MOA	[C], uM	Corr., r
(R)-Roscovitine	CDK1/2/5/7/9	ATP	20.00	**0.83**
AT7519	CDK 1/2/4/6/9	ATP	0.25	**0.87**
AZD 5438	CDK 1/2/9	ATP	2.20	**0.76**
BMS-265246	CDK 1/2	ATP	1.70	**0.9**
Cdk2 Inhibitor II	CDK 2	ATP	2.20	**0.74**
Dinaciclib	CDK2/5/1/9	ATP	0.03	**0.88**
DRB	CDK7/8/9 and CKII	ATP	20.00	**0.86**
Flavopiridol	CDK 1/2/4/6	ATP	0.25	**0.92**
NU 6140	CDK2, Aurora B/A	ATP	6.70	**0.79**
PD 0332991	CDK 4/6	ATP	15.00	**0.82**
Purvalanol A	CDK 1/2/5	ATP	6.70	**0.76**
R547	CDK 1/2/4	ATP	1.70	**0.82**
SU 9516	CDK 1/2/4	ATP	15.00	**0.88**

C Aurora

PKI	Target	MOA	[C], uM	Corr., *r*
Alisertib	Aurora A	ATP	15	**0.88**
CCT137690	Aurora A/B	ATP	0.2	**0.85**
PF-03814735	Aurora A/B	ATP	0.1	**0.89**
Tozasertib	Aurora A/C/B	ATP	2.2	**0.88**
ZM 447439	Aurora B/C/A	ATP	2.2	**0.85**

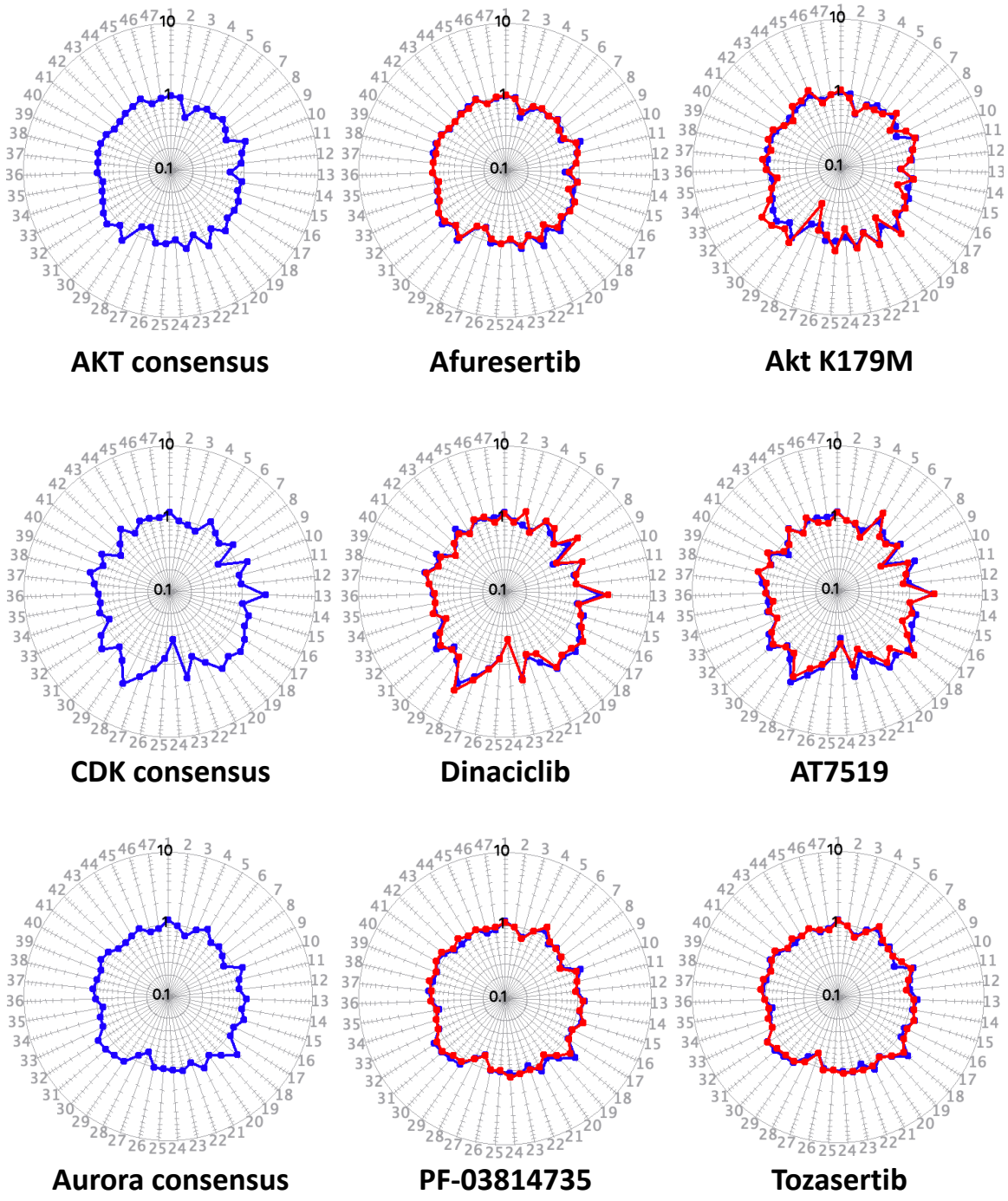

RTU #	Name
1	TGFRE
2	HNF6
3	TCF
4	Ebox
5	PPAR
6	NF1
7	GR
8	AP-1
9	ISRE
10	MTF-1
11	STAT3
12	TAL
13	NF-κB
14	FoxA2
15	CMV
16	Xbp1
17	CREB
18	AhR
19	EGR
20	NRF2
21	TA
22	ER
23	Oct
24	LXR
25	HSF-1
26	SREBP
27	p53
28	BMPRE
29	Pax6
30	HIF-1α
31	VDR
32	ROR
33	Ets
34	GLI-1
35	NRF1
36	GATA
37	E2F
38	C/EBP
39	Myb
40	PBREM
41	FXR
42	AP-2
43	RAR
44	FoxO
45	SOX
46	Sp1
47	Myc

Figure 1

A

Raf

PKI	Target	MOA	[C], uM	Corr., *r*
AZ 628	pan-Raf	ATP	60.00	**0.91**
Encorafenib	B-Raf	ATP	2.20	**0.88**
PLX4720	B-Raf	ATP	60.00	**0.74**
RAF265	pan-Raf	ATP	0.74	**0.95**
Regorafenib	pan-Raf multikinase	ATP	0.27	**0.87**
Sorafenib	pan-Raf multikinase	ATP	0.27	**0.77**
Vemurafenib	pan-Raf multikinase	ATP	6.67	**0.83**

B

MEK

PKI	Target	MOA	[C], uM	Corr., *r*
Binimetinib	MEK1/2	Allost.	2.2	**0.94**
PD 0325901	MEK1/2	Allost.	5	**0.69**
Selumetinib	MEK1,ERK1/2	Allost.	0.24	**0.95**
Trametinib	MEK1/2	Allost.	0.24	**0.98**

C

ERK

PKI	Target	MOA	[C], uM	Corr., *r*
GDC-0994	ERK1/2	ATP	0.027	0.93
Ulixertinib	ERK1/2	ATP	0.027	0.90

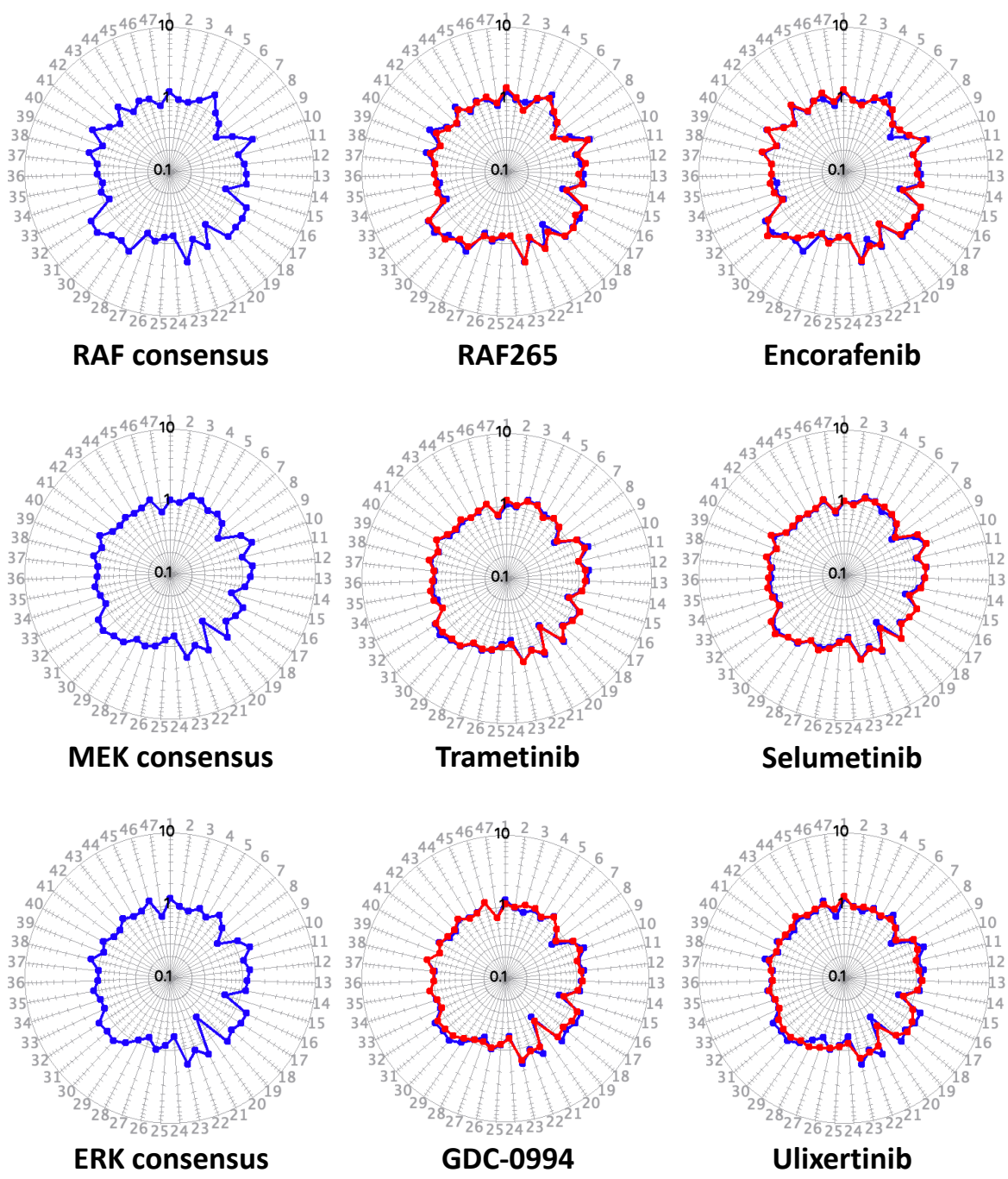

RTU #	Name
1	TGFRE
2	HNF6
3	TCF
4	Ebox
5	PPAR
6	NF1
7	GR
8	AP-1
9	ISRE
10	MTF-1
11	STAT3
12	TAL
13	NF-κB
14	FoxA2
15	CMV
16	Xbp1
17	CREB
18	AhR
19	EGR
20	NRF2
21	TA
22	ER
23	Oct
24	LXR
25	HSF-1
26	SREBP
27	p53
28	BMPRE
29	Pax6
30	HIF-1α
31	VDR
32	ROR
33	Ets
34	GLI-1
35	NRF1
36	GATA
37	E2F
38	C/EBP
39	Myb
40	PBREM
41	FXR
42	AP-2
43	RAR
44	FoxO
45	SOX
46	Sp1
47	Myc

Figure 2

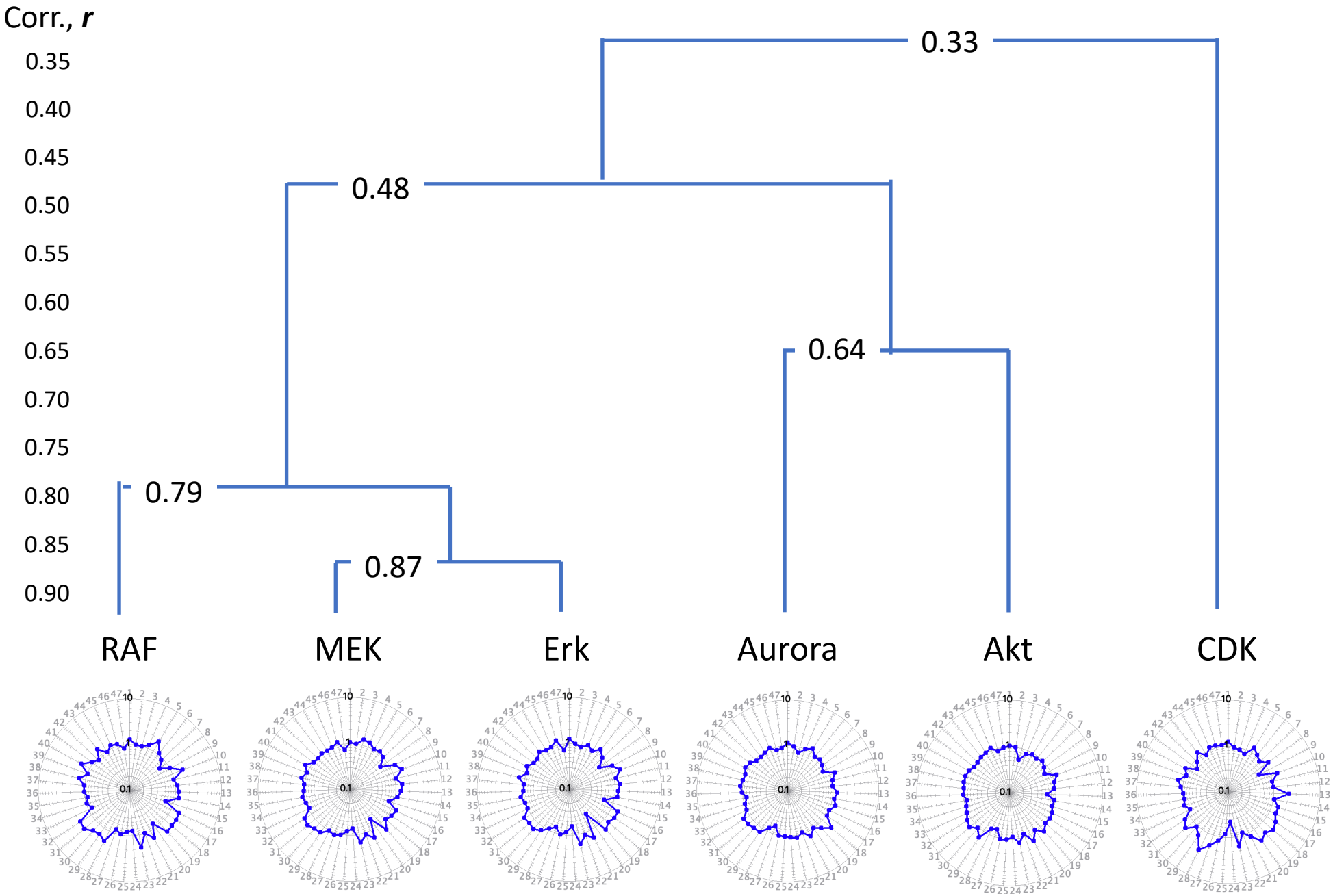
Corr., r
0.35
0.40
0.45
0.50
0.55
0.60
0.65
0.70
0.75
0.80
0.85
0.90
0.33
0.48
0.64
0.79
0.87
RAF
MEK
Erk
Aurora
Akt
CDK

Figure 3

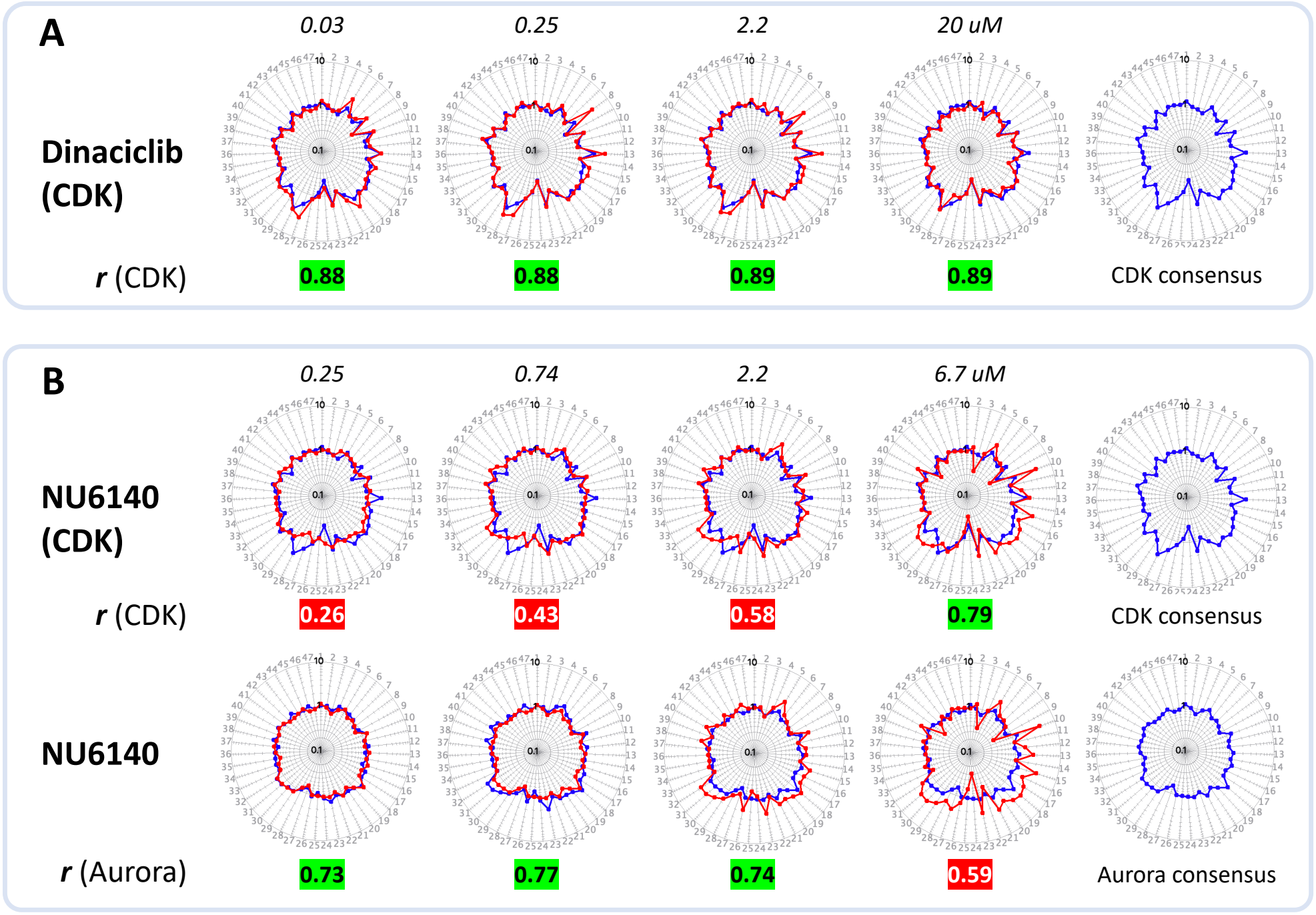
A
0.03
0.25
2.2
20 uM
Dinaciclib (CDK)
r (CDK)
0.88
0.88
0.89
0.89
CDK consensus
B
0.25
0.74
2.2
6.7 uM
NU6140 (CDK)
r (CDK)
0.26
0.43
0.58
0.79
CDK consensus
NU6140
r (Aurora)
0.73
0.77
0.74
0.59
Aurora consensus

Figure 4

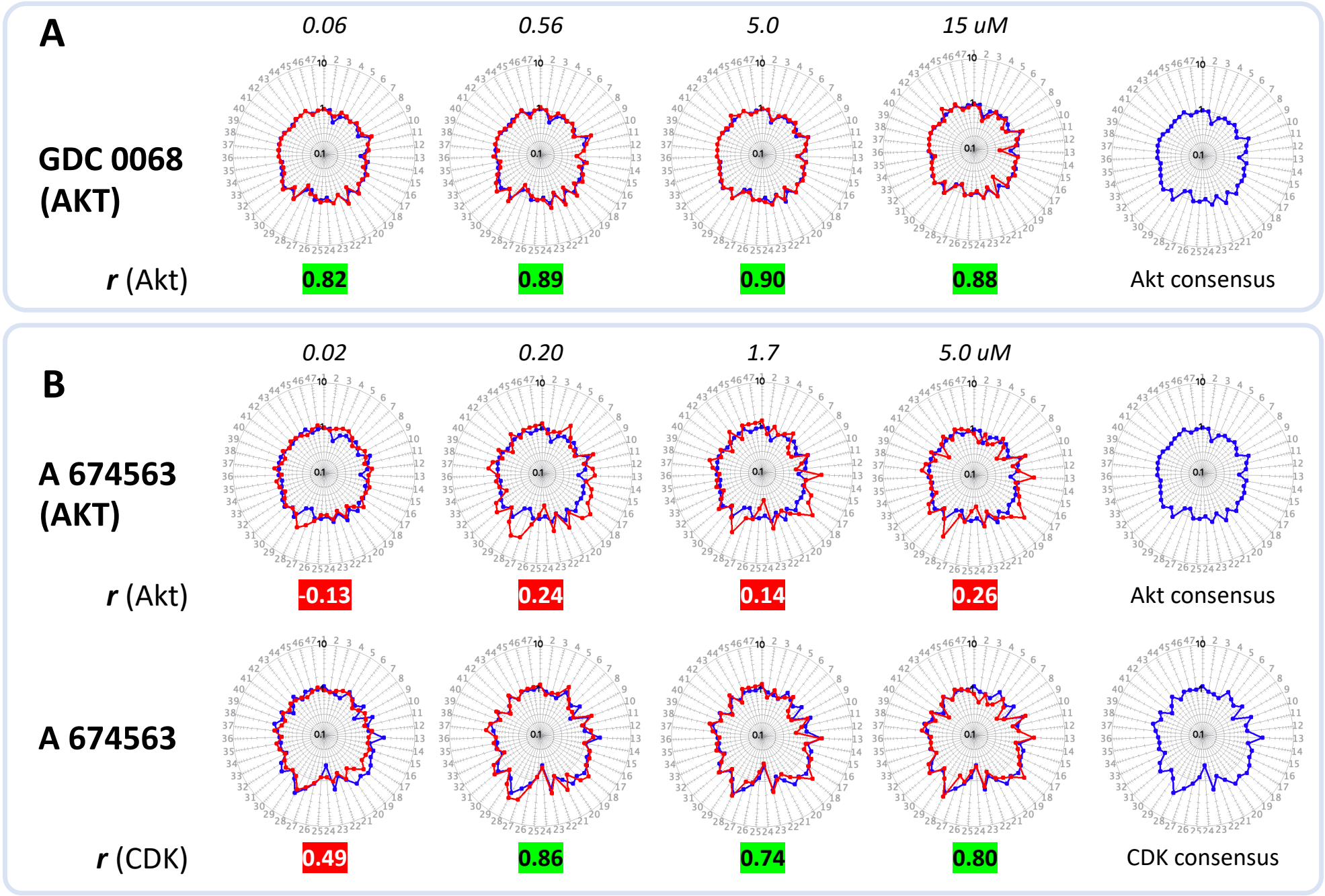
A
0.06
0.56
5.0
15 uM
GDC 0068
(AKT)
r (Akt)
0.82
0.89
0.90
0.88
Akt consensus
B
0.02
0.20
1.7
5.0 uM
A 674563
(AKT)
r (Akt)
-0.13
0.24
0.14
0.26
Akt consensus
A 674563
r (CDK)
0.49
0.86
0.74
0.80
CDK consensus

Figure 5

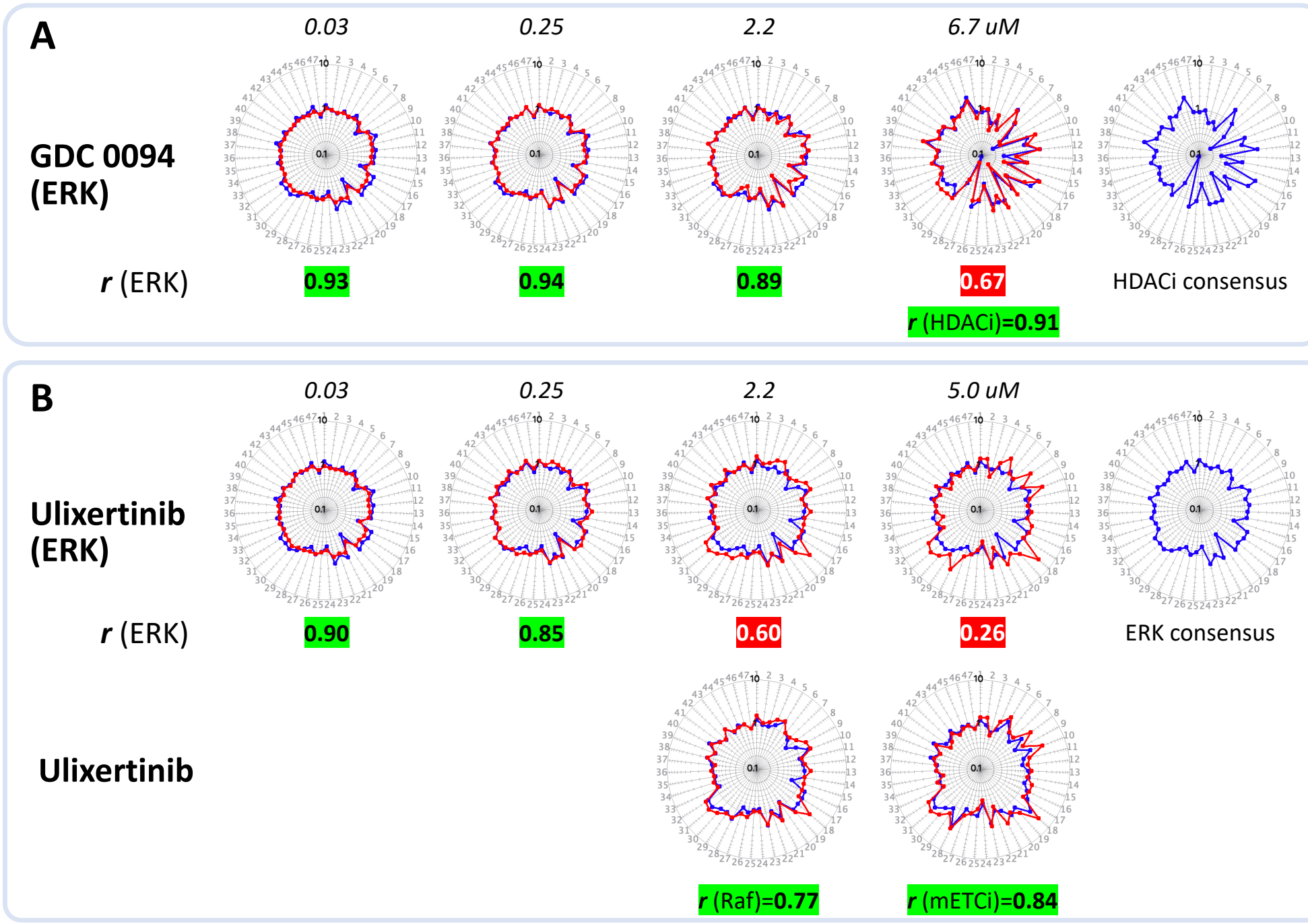
A
0.03
0.25
2.2
6.7 uM
GDC 0094 (ERK)
r (ERK)
0.93
0.94
0.89
0.67
HDACi consensus
r (HDACi)=0.91
B
0.03
0.25
2.2
5.0 uM
Ulixertinib (ERK)
r (ERK)
0.90
0.85
0.60
0.26
ERK consensus
Ulixertinib
r (Raf)=0.77
r (mETCi)=0.84

Figure 6

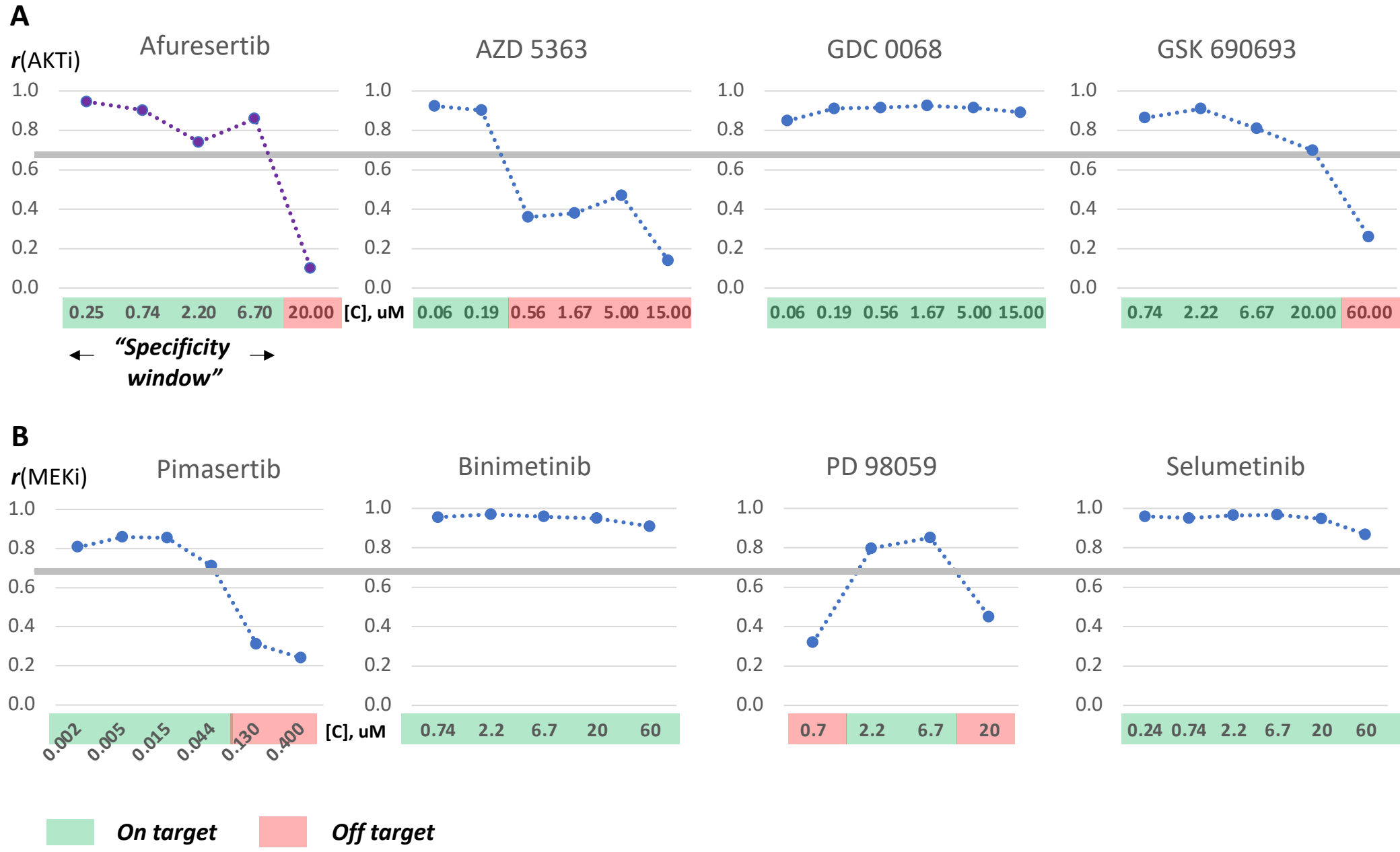
A
r(AKTi)
Afuresertib
AZD 5363
GDC 0068
GSK 690693
1.0
0.8
0.6
0.4
0.2
0.0
0.25 0.74 2.20 6.70 20.00
[C], uM
0.06 0.19 0.56 1.67 5.00 15.00
0.06 0.19 0.56 1.67 5.00 15.00
0.74 2.22 6.67 20.00 60.00
"Specificity window"
B
r(MEKi)
Pimasertib
Binimetinib
PD 98059
Selumetinib
0.002 0.005 0.015 0.044 0.130 0.400
[C], uM
0.74 2.2 6.7 20 60
0.7 2.2 6.7 20
0.24 0.74 2.2 6.7 20 60
On target
Off target

Figure 7